water

MDPI

Article

Porous Asphalt Mixture with Improved Fatigue Resistance and Stormwater Pollutant Reduction in Urban Road Pavement

Gabriela Hammes and Liseane Padilha Thives *

Department of Civil Engineering, Campus Florianópolis, Federal University of Santa Catarina, Florianopolis 88040-900, Brazil; gabrielahammes.ecv@gmail.com
* Correspondence: liseane.thives@ufsc.br; Tel.: +55-48-37212114

Abstract: One alternative measure to minimise the stormwater runoff volume and its pollutants and reduce impervious areas is to use permeable pavement. However, due to weak mechanical performance under heavy-load traffic related to fatigue resistance, porous mixtures and permeable pavements have restricted applications, i.e., parking lots and low-traffic roads. This work aims to evaluate the fatigue resistance of a porous asphalt mixture produced with highly modified asphalt (HiMA) and its potential contribution to reducing stormwater runoff and pollutants. In order to estimate the capability of runoff pollutants and stormwater flood reduction, a case study was performed on an urban road. A permeable pavement was designed using the porous mixture as a surface layer. The mixture volumetric parameters and asphalt content were established using the Marshall method, considering the void content, interconnected voids, permeability, Cantabro test, and moisture damage test evaluation. The resilient modulus and fatigue resistance tests were performed on a diametral compression device. The mixture design resulted in an asphalt content of 5.1% and a void content of 21.5%. The resilient modulus was 2764 MPa, and the porous mixture obtained excellent fatigue performance, allowing its application in diverse traffic conditions. The porous mixture efficiency infiltration capacity was 90%, and some runoff pollutants could be reduced after being filtered by the pavement surface, contributing to minimizing environmental contamination. This work filled part of a gap in predicting porous mixtures' fatigue performance, collaborating to popularise and expand its use for various purposes.

Keywords: stormwater; porous mixture; fatigue resistance; runoff; pollutants

Citation: Hammes, G.; Thives, L.P. Porous Asphalt Mixture with Improved Fatigue Resistance and Stormwater Pollutant Reduction in Urban Road Pavement. *Water* **2023**, *15*, 2962. https://doi.org/10.3390/w15162962

Academic Editor: Andrea G. Capodaglio

Received: 19 July 2023
Revised: 13 August 2023
Accepted: 15 August 2023
Published: 17 August 2023

1. Introduction

The surface waterproofing, resulting from cities' disorganised urban occupation, causes impacts on the environment, mainly related to changes in the hydrological cycle, and leads to flooding during heavy rainfall [1]. As for infrastructure, in urban centres, impermeable surfaces used for the road system and parking can represent up to 30% of the drainage basin area [2]. This study adopted the terms "permeable" to refer to pavement and "porous" to refer to the surface pavement layer.

Some water management strategies have been applied to minimise urbanisation's effects on the hydrological cycle. Retention reservoirs are employed in Brazilian (São Paulo and Rio de Janeiro) and French (Paris) cities to mitigate this problem. However, this alternative requires large areas, which are often unavailable and expensive [3,4]. Another viable option is the use of permeable pavements to reduce stormwater runoff volume, which is considered an unconventional alternative [5]. The stormwater infiltrates over the permeable pavements, crosses the draining layers, and can be stored for reuse or percolate into the soil to feed groundwater systems [6,7].

On a Nanjing (China) road, Zhu et al. [8] simulated different pavement structures under different rainfall conditions to evaluate the reduction of surface runoff and urban stormwater. They concluded that the permeable pavement could reduce surface runoff by more than 50%, and the percentage of flood peaks decreased as the surface layer thickness increased. Suripin et al. [9] measured the capacity of permeable pavement to reduce stormwater runoff in a parking lot. They proved that permeable pavements could decrease surface runoff volume by 33.42% to 46.05%.

Shafique et al. [10] monitored a permeable interlocking concrete pavement system to evaluate its effectiveness in controlling rainfall runoff in the field. They performed measurements on the stretch for four months. In conclusion, the authors observed that the permeable interlocking concrete pavement could decrease the runoff volume by 30% to 65% during storm events and reduce the increase in concentration time, which is an essential factor in lowering flash flooding in urban areas.

Infante et al. [11] measured the retention capacity of three porous mixtures, varying the composition, aggregates, and asphalt content. The void content of the mixtures was 28% (mixture A), 25% (mixture B), and 12% (mixture C). A rainfall simulator was used to reproduce different rainfall intensities (5, 10, 20, and 30 mm/h) and evaluate the runoff reduction. The authors concluded that the retention capacity of the porous mixtures arose between 85% and 20% and stated that higher values were observed for low-intensity rain. The mixtures with higher void content (A and B) had similar behaviour, and mixture C had less performance, proving that the low void content negatively affects the retention capacity.

Kuruppu et al. [12] stated that the practise of managing permeable pavement systems still needs to be improved due to a lack of in-depth scientific knowledge and economic uncertainties, and further studies are needed. One of the gaps in knowledge to be filled is related to surface layer mechanical resistance.

During in-service life, flexible pavements are subjected to repeated traffic loading and weather conditions variations, such as temperature, rain, and freezing, resulting in distress. Fatigue cracking is one of the most common pavement distress types and remains a significant challenge for pavement design [13]. Yang et al. [14] added that the cracking of flexible pavement is accelerated by precipitation-led moisture penetration associated with traffic loads.

In the fatigue failure process, the cracking initiates at the bottom of the surface layer, where the tensile stress or strain is highest, and then propagates to the top of the surface layer. Initially, as one or more longitudinal cracks propagate and after repeated traffic loading, the cracks connect and form many-sided structures, similar to the skin of an alligator, which is the final stage of fatigue distress [15,16].

Fatigue resistance can be defined as the asphalt mixture's ability to resist repeated traffic loading without significant cracking. The asphalt mixture's fatigue resistance is measured through tests like simple flexure, direct uniaxial, and diametral load tests [17].

For several years, a consensus was that only asphalt mixtures with low void volume and that were considered impermeable performed adequately in the field as pavement surfaces. Fatigue resistance is critical when a porous mixture is the pavement surface layer, reducing its durability [18]. Due to the large and interconnected air voids, this mixture is fragile in supporting the repeated traffic loading and thus more subject to fatigue cracking [19].

The high void volume allows the water to percolate and infiltrate inside the surface layer; the water reduces the adhesion between the asphalt and the aggregates, leading to moisture damage and reducing the layer's lifespan [20]. Other researchers corroborated that as porous mixtures are constantly exposed to oxygen and moisture due to their open structure, the ageing process contributes to cracking by fatigue [21–23].

Due to the high voids content (18% to 25%) and the consequent lower mechanical resistance to traffic stress, porous asphalt mixture applied as a surface layer is most commonly used in parking lots, patios, sidewalks, bike lanes and light traffic lanes [24].

The porous mixture's durability enhancement and fatigue resistance improvements can be achieved using modified asphalts [23]. Some authors have confirmed the porous asphalt mixtures' mechanical performance improvements through the introduction of fibres [25–27] or fatty acid amides [28] and by using modified asphalts, such as epoxy [29], polyurethane [30], rubber from waste tires [31], and styrene butadiene styrene—SBS [32–34].

Asphalts modified by SBS have been widely used in producing porous mixtures whose contents vary from 2% to 3%. On the other hand, to provide a network of polymer chains and improve the mixture's mechanical performance, especially subject to heavy traffic and higher temperature conditions, an asphalt with the introduction of higher levels of SBS (7% to 8%), called Highly Modified Asphalt (HiMA), was developed [35].

Zhang et al. [36] evaluated the mechanical performance of porous asphalt mixtures and tested four SBS polymer contents in asphalt modification (4.5%, 6.0%, 7.5%, and 9.0%). The authors concluded that increasing the SBS content improved resistance to disintegration, moisture damage, fatigue, and permanent deformation of the mixture. However, it was noticed that the increase in fatigue life was more significant from 6.0% to 7.5% than between 7.5% and 9.0% of SBS content, indicating that the continuous increase of SBS content would produce a limited improvement in the fatigue performance of the porous mixtures.

The design requirements for porous asphalt mixtures differ from those commonly established for conventional mixtures. Hamzah et al. [37] proposed a design method to select the asphalt content based on four control parameters: permeability coefficient (K), void content, abrasion loss, and binder draindown. In Brazil, Kolodziej [38] established the asphalt content of porous mixtures by considering void content, interconnected voids, and the Cantabro test results. Ji et al. [39] asserted that the permeability coefficient of the porous mixture was a parameter that influenced the pavement drainage performance.

There are some differences among standards-settled requirements for porous asphalt mixtures. A brief comparison between the North American ASTM D7064 [40] and the Brazilian standard DNER-ES 386 [41] is presented. The ASTM standard [40] establishes, for porous mixtures, a minimum of 18% void content, while the DNER [41] standard sets a range between 18% and 25%. In the Cantabro test, the DNER [41] limits mass loss to 25% and the ASTM [40] to 20%. As for mechanical performance, in Brazil, a minimum tensile strength of 0.55 MPa is required by a diametral compression test (temperature of 25 °C). The North American specification requires that the tensile strength ratio be at least 80% and the maximum draindown be 0.3%. The Brazilian standard also recommends that the asphalt content fit between 4.0% and 6.0%; however, the mixture design must be accomplished.

Dan et al. [19] stated that, generally, the research on porous asphalt mixtures primarily focuses on the mixture design and mechanical behaviour; usually, permanent deformation resistance is evaluated. However, the authors confirmed that the porous mixture's fatigue performance must be measured, especially considering that such mixtures' performance is severely affected by moisture damage.

The stormwater runoff contains several pollutants that are directly carried to drainage systems during rain events. Consequently, urban runoff is one of the ways to transfer pollutants to the aquatic and marine environment [42]. The primary contaminants of urban runoff are heavy metals, solids, organic micropollutants, pathogenic microorganisms, nutrients, and microplastics [43,44].

Several studies have proved that porous surface layers and permeable pavement can reduce the concentration of some stormwater runoff pollutants [45–49]. Research demonstrated that total suspended solids, ammonia, nitrate, total phosphorous, and chemical oxygen demand were removed only by the porous surface pavement layer before the stormwater was passed through other pervious layers [50]. Liu et al. [51] confirmed that adding alternative fillers (diatomite, quartz sand, and straw biochar) in the porous asphalt mixture can enhance the removal effect of dissolved pollutants, especially heavy metals. They also found that the total removal of suspended solids increased by 60% to 80%.

This work proposes to produce a porous asphalt mixture with highly modified asphalt (HiMA) to improve fatigue resistance. The mixtures were designed using Marshall methodology with four asphalt contents (4.5%, 5.0%, 5.5%, and 6.0%). In order to define the asphalt content, the samples were submitted to tests such as void content, interconnecting voids, permeability, Cantabro, and moisture-induced damage. Then, the porous mixture mechanical tests were performed through the indirect tensile test to evaluate the resilient modulus and fatigue resistance. A pavement structure was designed to evaluate the potential use of the porous mixture under high-traffic conditions related to fatigue resistance. Moreover, the porous mixture's filtering capacity was measured using models exposed to rain events. The porous mixture's ability to reduce runoff pollutants was also assessed.

The ability to filter stormwater pollutants can contribute to environmental protection and runoff reduction in urban areas. In addition, the fatigue performance investigation represents an advancement in porous mixture study and enhances its application in high-load traffic conditions. This work's novelty was to design a porous asphalt mixture with outstanding fatigue resistance using highly modified asphalt.

2. Materials and Method

The method encompassed the asphalt porous mixture design to obtain the asphalt content. After that, the porous mixture samples were produced and submitted to mechanical tests (resilient modulus and fatigue). The porous asphalt mixture's infiltration capacity was evaluated using models to estimate the runoff reduction. The water from runoff was collected on an urban road after rain events, and the pollutants in the water were measured (before and after filtering through the models). Considering the urban road case study, a pavement structure was designed to establish the life span related to fatigue performance and runoff and pollutants reduction.

2.1. Materials and Mixture Design

The granitic aggregates were obtained from Santa Catarina State, Southern Brazil, and consist of the following nominal sizes: (i) grade 1: 4.8 mm to 9.5 mm; (ii) grade 2: inferior to 4.8 mm (stone powder). The aggregates were characterised according to the Brazilian specification tests [41] and were adequate for producing asphalt mixtures (Table S1—Supplementary Data). The mixture gradation curve adopted was the same one used by Lu et al. [52], as shown in Figure 1.

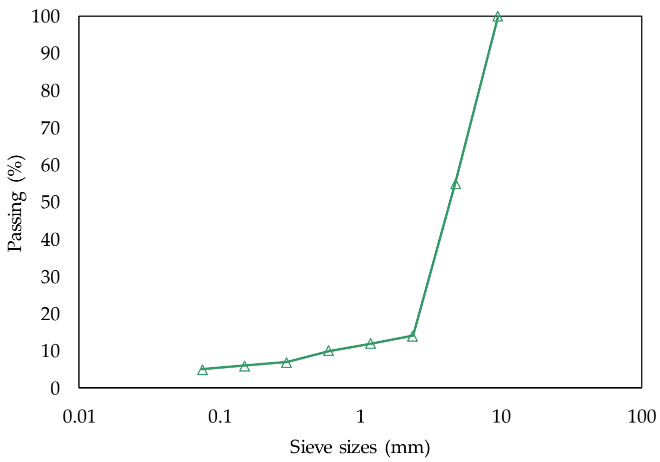

Figure 1. Mixture gradation curve.

A Highly Modified Asphalt (HiMA) supplied by a Brazilian distributor was used to produce the porous mixture. HiMA was made with the base asphalt PEN 50/70 (classified by penetration grade) and styrene-butadiene-styrene (SBS), whose amount of polymer SBS added is more significant than 7% (both the modification process and the exact percentage of SBS are protected by industrial confidentiality). As HiMA still has no standard specification in Brazil, the tests commonly used for modified asphalt characterisation were performed. As a result, HiMA fits into the Brazilian requirements for modified asphalts [53], as shown in Table 1.

Table 1. HiMA characterisation tests results.

Test	Unit	Result	Reference
Penetration, 100 g, 5 s, 25 °C	0.1 mm	36	[54]
Softening point [1]	°C	90.8	[55]
Elastic recovery, 20 cm; 25 °C	%	95	[56]
Apparent viscosity [2]			
135 °C, spindle 21, 20 rpm	cP	2989	
150 °C, spindle 21, 50 rpm	cP	1408	[57]
175 °C, spindle 21, 100 rpm	cP	405	
Storage stability, ΔSp [3]	°C	2.1	[58]
RTFO [4]			
Mass loss	%	0.333	[59]
Change in softening point	°C	4.3	[55]
Change in elastic recovery	%	97.8	[56]
Retained penetration	%	68	[54]

Note(s): [1] Ring-and-ball method; [2] Brookfield viscometer; [3] Softening point difference; [4] Rolling Thin Film Oven.

The porous mixture samples production followed the Brazilian standard [41] to evaluate the asphalt content. Marshall samples (three for each content) were prepared with four asphalt contents (4.5%, 5.0%, 5.5%, and 6.0%), resulting in twelve compacted samples (Figure S1—Supplementary Data). Before compaction, the mixtures were maintained in an oven at 150 °C for two hours to simulate the short-term ageing representing the production, transport, and compaction at the construction site. Samples with a diameter of 100 mm and a height of 65 mm were moulded by applying 50 blows per side. From the viscosity-temperature curve, the following temperature ranges were established: (i) asphalt heating: 160 °C to 165 °C; (ii) aggregate heating: 175 °C; (iii) mixture compaction: 150 °C. After that, all samples were submitted to the following tests: (i) void content; (ii) interconnecting voids; (iii) permeability; and (iv) Cantabro. The asphalt content was defined based on such tests and resulted in two contents; then, one was chosen based on the moisture-induced damage test result.

The void content was calculated using Equation (1), following the ASTM D3203 standard [60]. According to the Brazilian specification [41], the range of void content must be between 18% and 25%. The interconnected voids were estimated according to Equation (2) (AFNOR NF P98-254-2 standard [61]). The test measures the amount of the film of water kept constant for ten minutes on the upper face of the sample while the other faces are maintained waterproofed. Raimbault et al. [62] considered that the interconnected voids should be at least 12% and not greater than 20%, and such limits were adopted in this study as a selection criterion.

$$\mathrm{Vc} = [(\mathrm{G_{mm}} - \mathrm{G_{mb}})/(\mathrm{G_{mm}})] \times 100 \tag{1}$$

where Vc is the void content (%), G_{mm} is the theoretical maximum specific gravity of the mixture (g/cm^3), and G_{mb} is the bulk specific gravity of the mixture (g/cm^3).

$$\mathrm{Iv} = [(\mathrm{M_{ab}})/(\mathrm{A_f} \times \mathrm{h_{red}})] \times 100 \tag{2}$$

where Iv is the interconnected void content (%); M_{ab} is the mass of absorbed water (g); A_f is the upper face area (cm^2), and h_{red} is the reduced height (cm), which is calculated using Equation (3).

$$\mathrm{h_{red}} = \mathrm{h_m} - (\mathrm{d_{max}}/20) \tag{3}$$

where h_{red} is the reduced height (cm), h_m is the average of three measurements of the sample height (cm), and d_{max} is the maximum aggregate size (cm).

The permeability coefficient (K) was measured by a falling head permeameter LCS, according to the standard NLT-327 [63] and Equation (4). The time required for a column of water with standardised height to infiltrate the sample is measured in the test. Due to the sample form and dimensions, the standard test was adapted to direct the water flow through the sample (Figure 2).

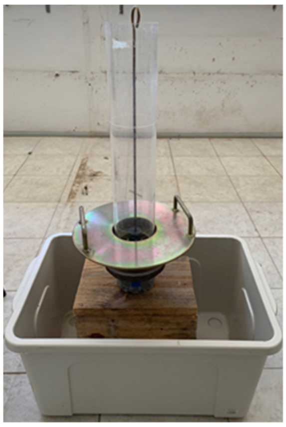

Figure 2. Adapted permeability test.

The permeability coefficient of each sample was calculated from the average of three measurements.

$$\ln K = 7.624 - 1.348 \times \ln T \quad (4)$$

where K is the permeability coefficient (cm/s) and T is the water flow time (cm).

The Cantabro test measures the breakdown of compacted samples, expressed by the loss of mass percentage, after the abrasion test in the Los Angeles machine (LAM). Initially, the samples were compacted at the design asphalt content, gradation, and air voids. Before the Cantabro test, the samples were conditioned in an oven at 25 °C for six hours, and the mass of each sample was measured (the initial mass). The test was performed using one sample at a time. The sample was placed into the LAM drum without the steel balls and subjected to 300 revolutions at 30 to 33 rpm. After 300 revolutions, the loose material, broken off from the sample during the test, was discarded, and the mass was measured (the final mass). The Cantabro test was performed according to the Tex-245F [64] standard, and the Cantabro Loss was calculated using Equation (5). The resistance to moisture-induced damage was evaluated in compacted samples and followed the AASHTO T 283 standard [65]. The tensile strength was calculated using Equation (6) and the tensile strength ratio using Equation (7).

$$CL = [(A - B)/A] \times 100 \quad (5)$$

where CL is the Cantabro Loss (%), A is the initial mass of sample (g), and B is the final mass of the sample (g).

$$TS = 2000 \times P/(\pi \times t \times D) \quad (6)$$

where TS is the tensile strength (kPa); P is the maximum load (N); t is the sample thickness (mm); and D is the sample diameter (mm).

$$TSR = (S_2/S_1) \times 100 \quad (7)$$

where TSR is the Tensile Strength Ratio (%); S_1 is the average tensile strength of the dry subset (kPa); and S_2 is the average tensile strength of the conditioned subset (kPa).

2.2. Mechanical Tests

After selecting the asphalt content, samples were produced for mechanical tests (resilient modulus and fatigue resistance). The resilient modulus test followed the DNIT 135 standard [66], an indirect tensile test in controlled force mode at 25 °C, in which the samples were submitted to 0.1 s loading and 0.9 s rest periods. The resilient modulus was calculated using Equation (8). The fatigue resistance was evaluated through a repeated load-controlled force indirect tensile test (standard DNIT 183 [67]), the most commonly used in Brazil. The tests were performed on the same equipment to obtain the resilient modulus. The test conditions were a haversine loading wave, a frequency of 1 Hz, and a temperature of 25 °C. Four tension levels (20, 25, 30, and 35% of tensile strength) were applied, and three samples were tested at each level. The fatigue curve is represented by Equation (9).

$$RM = [P/(\Delta H \times t)] \times (0.2692 + 0.997\nu) \quad (8)$$

where RM is the Resilient Modulus (MPa); P is the cyclic load (N); ΔH is the horizontal displacement (elastic or resilient) (mm); t is the sample height (mm); and ν is the Poisson's coefficient (taken as 0.30).

$$N = k_1 \times \sigma^{-k}{}_2 \quad (9)$$

where N is the cycle number; σ is the tensile strain (microstrain); and k_1 and k_2 are the experimental coefficients.

2.3. Porous Mixture Infiltration Capacity

The infiltration capacity of the porous mixture was measured using models exposed to rain events. Three acrylic boxes were constructed with the following dimensions: 50 cm × 18 cm internal base and 53 cm height. Two compacted porous mixture slabs (50 cm × 18 cm) were assembled in two acrylic boxes, supported by metal grids, while an empty box was the control. All models were exposed to the same rain events. After each rain event, the water infiltrated and stored in the boxes was measured using a graduated rule. The water stored in the empty box was also measured to evaluate the total rainwater volume. The infiltration capacity for each slab was obtained by comparing the water infiltrated after passing by the slabs with the accumulated water in the empty box. The porous mixture infiltration capacity was obtained using Equation (10), calculated by the average of models.

$$E = (h_i/h_s) \times 100 \quad (10)$$

where E is the infiltration capacity (%), h_i is the height of rainwater infiltrated in the models (mm), and h_s is the height of rainwater stored in the empty box (mm).

2.4. Evaluation of Runoff Pollutant Reduction

At the first hour of rain events (four), stormwater runoff samples were collected in the gutters of the urban road (case study), and the water pollutants were measured. Part of the collected water was spilt over the models to evaluate the filtering capacity and retain pollutants. Then, the water quality, filtered by the models, was also measured. The chosen water quality parameters followed the National Water Agency's (ANA) [68] recommendations for non-potable purposes (Table S2—Supplementary Data).

2.5. Pavement Structure Design

A case study was conducted on an urban road for the porous asphalt mixture application. A pavement structure was designed using the Brazilian mechanistic-empirical pavement software, MeDiNa [69] (version 1.1.5.0), and the potential use of the porous mixture under high traffic conditions related to fatigue resistance was evaluated. In the pavement structure, it was considered that only the surface layer is porous and the others are non-pervious layers.

3. Case Study

Florianópolis (27.5948° S, 48.5569° W) is the Santa Catarina State capital (Figure 3), with most of the municipality located on an island. The climate zone is humid subtropical, with an average temperature of 21.1 °C [70]. The average monthly rainfall measured between 1991 and 2020 [71] is 147 mm, resulting in an accumulated annual precipitation of 1766 mm (Figure 4).

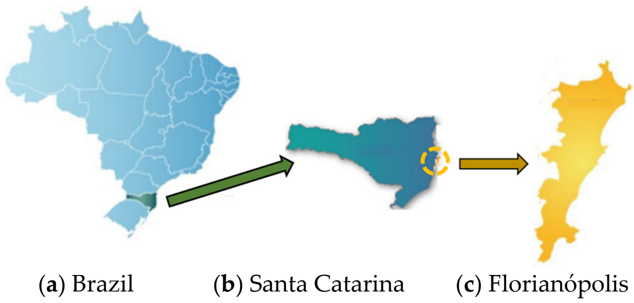

Figure 3. Location of Florianópolis in Brazil.

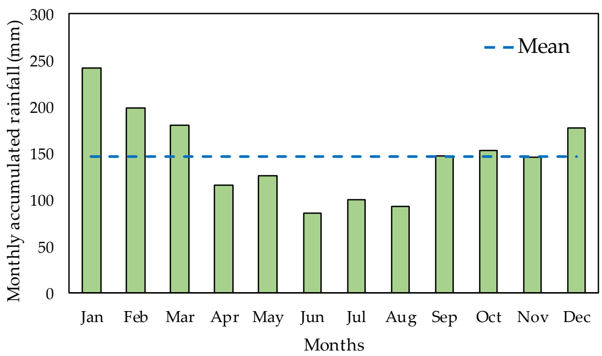

Figure 4. Monthly annual average rainfall in Florianópolis (Based on [71]).

One of the main arterial roads is located in the city's central region, whose layout follows the sea and a permanent preservation area, a mangrove (Figure 5, highlighted in blue). The road was built on an embankment in the 1960s and expanded in the 1980s. This essential road called Beira Mar Norte Avenue, provides access to the bridges to the mainland and connects the central neighbourhoods and the northern beaches. *Beira Mar* Avenue is 7000 m long (4700 m edges the sea and 2100 m edges the mangrove), composed of six lanes (three by traffic direction), each with a 3.50 m width. The pavement structure has a surface layer with a dense-graded hot mix (asphalt rubber) and a granular base.

In December 2022, the accumulated rainfall in Florianópolis was 460 mm, and on two consecutive days, there was rainfall of 123 mm and 137 mm [72]. Due to the heavy rains, several floods were observed on this road, as shown in Figure 6. However, there is a superficial drainage system along the road (kerb and gutter), which is sometimes insufficient depending on the intensity of the rain.

Figure 5. *Beira Mar* Avenue in Florianópolis.

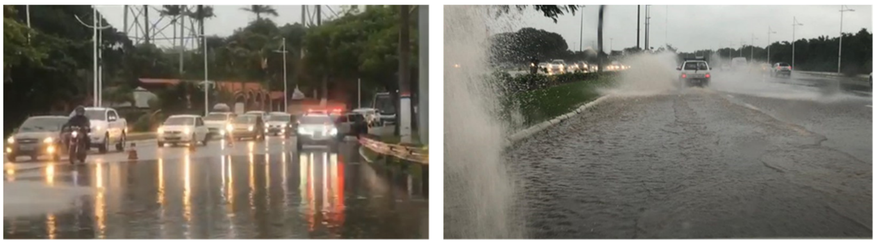

Figure 6. Floods on *Beira Mar* Avenue [73].

4. Results

4.1. Mixture Design

Due to the four asphalt contents (4.5%, 5.0%, 5.5%, and 6.0%), the samples were tested for void content, interconnected voids, permeability coefficient, and Cantabro Loss. Figure 7a shows that the minimum limit of 18% void content (dotted red line) was met for all asphalt contents tested. It was also observed that the void content decreased with the increase in asphalt content. However, between 5.5% and 6.0%, the void content remained almost constant, with a variation of less than 0.1%, changing from 20.6% to 20.5%, respectively. On the other hand, the interconnected voids, shown in Figure 7b, reduced due to the increasing asphalt content, more between 4.5% and 5.0%. All asphalt contents met the criteria adopted (between 12% and 20%, dotted red lines in Figure 7b).

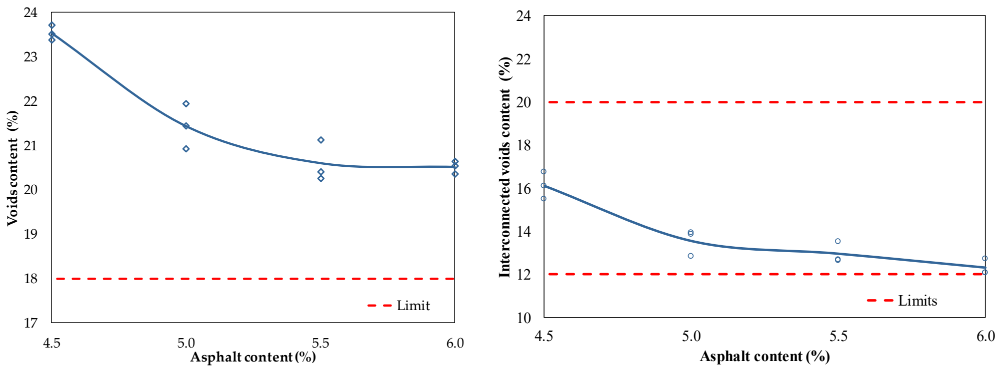

(**a**) Voids content (**b**) Interconnected voids

Figure 7. Voids as a function of asphalt content.

Higher K values were obtained for 4.5% (Figure 8a), and the trend observed was a reduction in the average permeability due to the asphalt content increase. The minimum K value (dotted red line in Figure 8a) of 0.12 cm/s was not met for the 5.5% and 6.0% asphalt contents. As for the Cantabro test, the mass loss was less than the maximum limit of 20% (dotted red line in Figure 8b) for all asphalt contents. On the other hand, the mass loss was greater between the contents of 4.5% and 5.0%, i.e., 13.1% and 8.8%, respectively. Only 4.5% and 5.0% of asphalt contents met the permeability coefficient criterion. The 5.0% content resulted in a lower mass loss in the Cantabro test (an average of 8.8%) and was adopted to conduct the moisture-induced damage test. However, for 5.0%, the results did not meet the standard's requirements, and it was necessary to perform the test for the asphalt content of 5.1%.

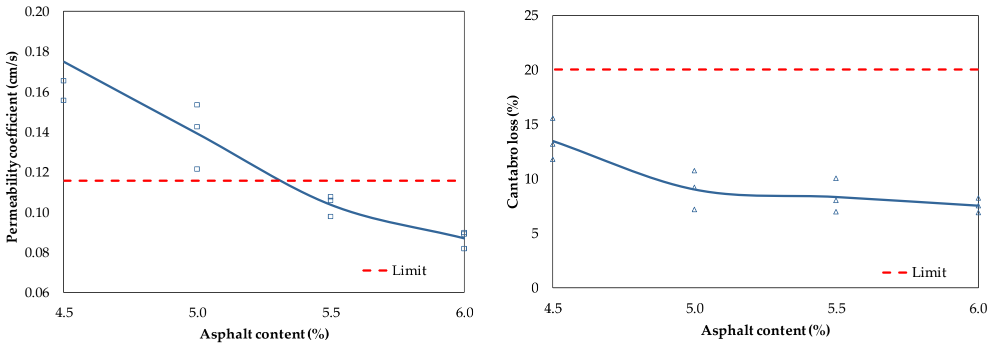

(**a**) Permeability (K) (**b**) Cantabro Loss (CL)

Figure 8. Parameters K and CL as a function of asphalt content.

Figure 9 shows the average tensile strength results for 5.0% and 5.1% (the dotted red line shows the minimum limit of 0.55 MPa [41]); both met the requirement (unconditioned samples). Figure 10 presents the average tensile strength results from the comparison obtained for conditioned and unconditioned samples.

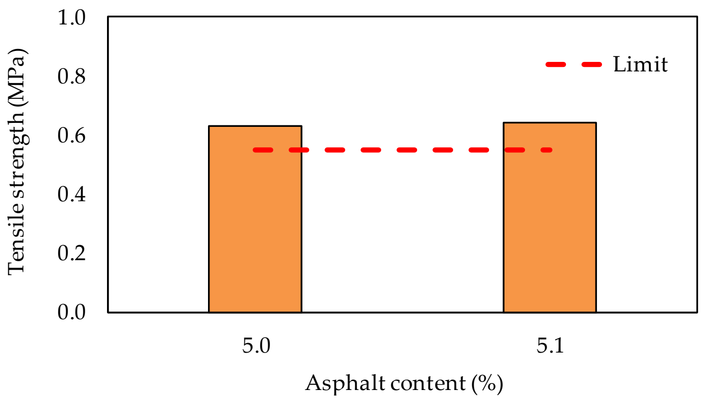

Figure 9. Tensile strength results.

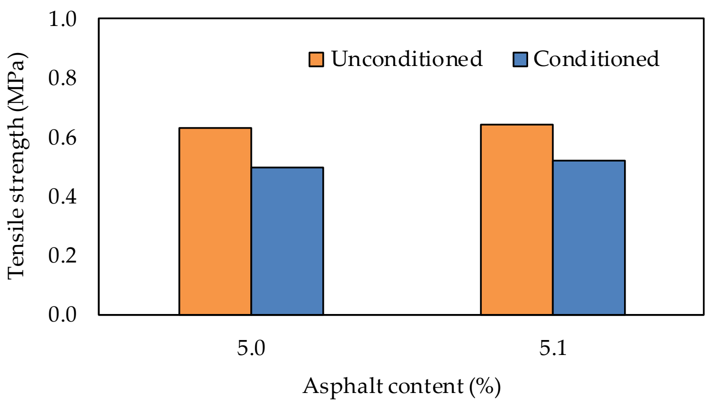

Figure 10. Tensile strength results for unconditioned and conditioned samples.

In addition, the tensile strength ratio of conditioned samples with an asphalt content of 5.0% was 78.8% (Figure 11), lower than the minimum required value of 80% [40]. The results of samples with 5.1% met the requirements, with a tensile strength of 0.64 MPa and a retained tensile strength of 80.8%. In this sense, the samples were produced with 5.1% asphalt content to perform the mechanical tests, for which the void content resulted in 21.5% and K, obtained by means of regression, in 0.13 cm/s.

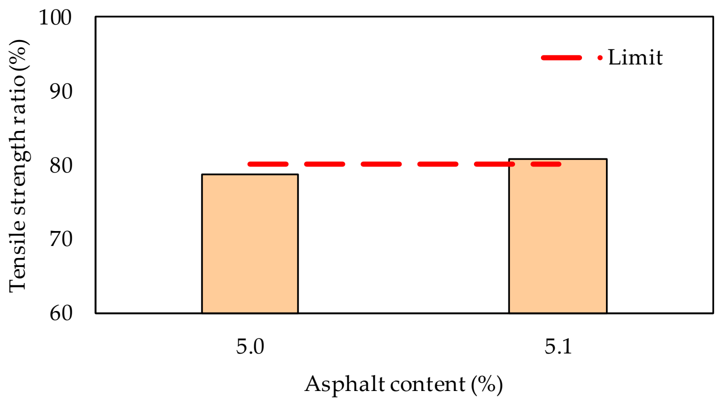

Figure 11. Tensile strength ratio results.

4.2. Mechanical Test Results

The resilient modulus (asphalt content of 5.1%) was obtained from the three samples' average, resulting in 2764 MPa (Table 2). Figure 12 shows a sample placed on the loading device during the test. The fatigue curve is presented in Figure 13, and the parameters obtained are shown in Table 3, related to Equation (9). Despite the high void content, the porous asphalt mixture's fatigue performance can be attributed to the HiMA asphalt.

Table 2. Resilient modulus results.

Parameters	**Sample** 1	2	3
Modulus (MPa)	2717	2797	2779
Mean (MPa)		2764	
Standard deviation (MPa)		42	
Coefficient of variation (%)		1.5	

Figure 12. Porous mixture sample positioned on the loading device in the fatigue test.

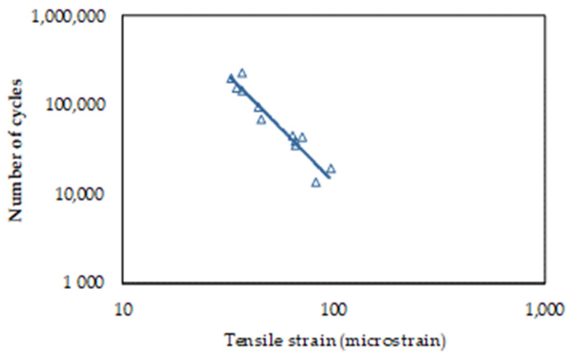

Figure 13. Porous asphalt mixture fatigue curve.

Table 3. Porous mixture fatigue parameters.

Parameters	Results
k_1	4.0×10^{-6}
k_2	2.391
R^2	0.93

4.3. Porous Mixture Infiltration Capacity

The porous mixture infiltration capacity results, measured through the models, are presented in Table S3 (Supplementary data). Even though the slabs presented the same granulometry, asphalt content, and void content, the aggregate arrangement during the compaction process can have a slight position variation that influences the interconnected voids. Thus, the water infiltration results can differ despite the slabs being subjected to the same rain events. For slab 1, the efficiency capacity resulted in 89.9% (a standard deviation of 5.2%), while for slab 2, it was 90.2% (a standard deviation of 4.5%). The results proved that the porous mixture presented a great infiltration capacity, and the result adopted was 90%.

4.4. Pollutants Reduction

The results of the evaluation of water quality collected from stormwater runoff (road) and filtered through the porous mixture slab are presented in Table S4 (Supplementary data), indicating that the porous mixture was relatively efficient in removing runoff pollutants.

On average, the porous mixture significantly reduced concentrations of total phosphorus (more than 400%), total suspended solids (975%), and faecal coliforms (more than 200%). Also, the water turbidity and colour decreased by 61.8% and 4.6%, respectively. The pH slightly varied (2.5%) and remained 6.8 to 7.5. The concentrations of ammoniacal nitrogen increased by 23.0% after being filtered by the porous mixtures. The retention capacity was imprecise for the concentrations of chemical oxygen demand, nitrate, and nitrite.

4.5. Pavement Design

The pavement structure (without infiltration) was designed for the urban road (case study) with porous asphalt as the surface layer using the software MeDiNa [69]. The pavement layer's properties (Table 4) were evaluated by Simm Júnior [74] and Custódio et al. [75]. The input MeDiNa parameters of the subgrade are presented in Table S5 (Supplementary Data).

Table 4. Pavement layer's properties.

Property	Layers			
	Surface	**Waterproofing**	**Base**	**Subgrade**
Material	Porous mixture	Asphalt mixture	Granular [2]	Soil [3]
Thickness (cm)	Design [1]	2.0	16.0	-
Modulus (MPa)	2764	1987	268	220
Poisson coefficient	0.30	0.30	0.35	0.45

Note(s): [1] Thickness is evaluated by the pavement design; [2] [74], [3] [75].

The required thickness of the porous mixture (surface layer) considering the pavement layers (Table 4) is presented in Figure 14, according to the equivalent single axle loads (ESALs). The life design was ten years, and the traffic was estimated at the standard ESAL of 80 kN.

Figure 14 shows that the designed porous mixture could be applied in more adverse traffic-load conditions due to its high fatigue resistance with thickness increases. It is important to emphasise that the pavement design did not consider the waterproofing layer's contribution in terms of resistance. The minimum surface layer thickness allowed by MeDiNa is 5.0 cm, which for this structure (Figure 15) results in an ESAL of 9.4×10^6.

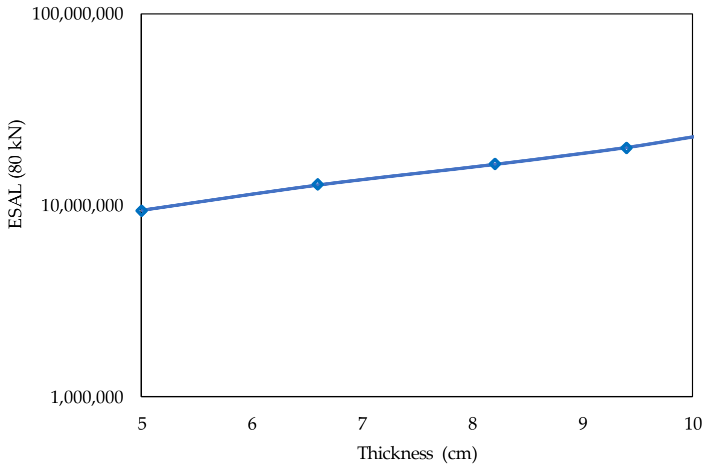

Figure 14. Porous asphalt mixture thickness required as a function of ESALs.

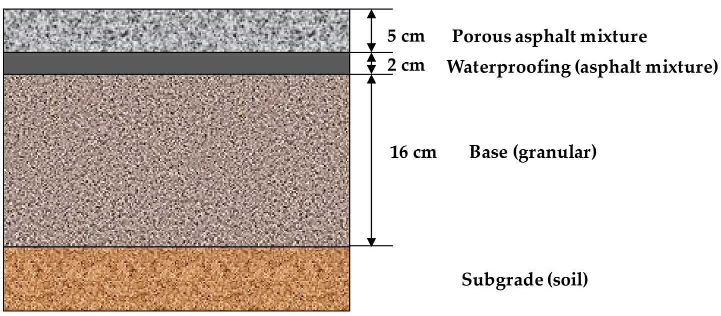

Figure 15. Pavement structure.

5. Discussion

Impermeable urban road pavement surfaces contribute to runoff volume increases and flooding potential in cities during storm events [76]. Zanoletti and Bontempi [42] added that floods are increasing due to climate change effects associated with waterproof surfaces in cities. Moreover, impervious surfaces assigned to urbanisation decrease the potential for groundwater recharge and promote flooding and drought cycles [77]. Previous studies showed that as impervious surfaces increased, infiltration rates decreased by 4–19%, evaporation rates rose by 0.2% to 1%, and stormwater runoff increased by 4% to 18% [78].

The efficiency of the drainage system depends on each region's regime, intensity, and duration of rainfall. This work evaluated a case study on an urban road in Florianópolis (Brazil), with higher rainfall in the summer (Figure 4). Due to frequent heavy rains in the city and impervious pavement surfaces associated with insufficient drainage, floods harm urban transport mobility, especially once the city is an island (Figure 6).

One of the best management practises for mitigating environmental impacts associated with floods, drainage controls, and urban stormwater runoff is permeable pavement use [79]. Permeable pavements are well suited for high-density urban areas with limited space. When properly designed, many benefits are associated, such as reducing runoff quantity and reducing pollutants in receiving water bodies. Infante et al. [11] corroborated that porous mixtures are effective in reducing surface runoff and can be an alternative to facing and managing urban flooding.

A challenge associated with permeable pavement use is related to the mechanical behaviour of porous mixtures (the surface layer). Although permeable pavements can withstand truckloads, they are generally unsuitable for applications in areas exposed to high-load traffic [80], and they are commonly used in parking lots, low-traffic roads, sidewalks, and driveways [81].

On the other hand, using modified asphalt contributed to the porous mixture's mechanical resistance improvements [25–34]. The high void content of the porous mixtures contributes to their weak fatigue performance, and the study to achieve better improvements remains a gap to be filled related to such mixtures.

In this scenario, the present work focused on the fatigue resistance evaluation of a porous asphalt mixture to provide a related reference for its potential performance under adverse load traffic. An asphalt highly modified by SBS (HiMA) was used to produce the porous mixture. The mixture design for asphalt content establishment comprised volumetric parameter measurements, such as void content and interconnected voids, associated with permeability, Cantabro, and moisture-induced damage test results.

The Cantabro tests were performed in porous mixtures with SBS and showed that mass loss was more significant than 20% after 100 revolutions in the Los Angeles machine for mixtures with a void content of 20%. For the porous mixture designed in this work, with 21.5% void content, after 300 revolutions, the mass loss was lower than 10.0%, which can be attributed to HiMA's capability to maintain adhered aggregates and provide mixture stability [82].

The mechanical tests were employed to measure the resilient modulus and fatigue curve parameters. The resilient modulus of the porous mixture, at 2764 MPa, can be considered high, as usually found for asphalt porous mixtures, suggesting that it was due to HiMA's contribution. Comparatively, for porous mixtures with similar void content and the tests conducted at the same temperature, the resilient modulus obtained was 1875 MPa for a mixture using asphalt modified by SBS [83] and 1483 MPa for a mixture with a cement additive [84].

Li et al. [29] conducted fatigue tests using a four-point bending beam device. They found that porous mixtures produced with asphalt modified by epoxy obtained fatigue resistance 2.0 to 4.5 times greater than a conventional mixture. However, porous mixtures were relatively sensitive to high strain levels. Fatigue tests with an indirect tensile device were performed in porous mixtures, proving that moisture damage significantly affects fatigue resistance. It was concluded that the material exhibited higher fatigue dependence on moisture damage at higher stress levels [19].

The asphalt mixture's fatigue resistance is one of the main factors indicative of pavement durability, but it is not frequently evaluated when the porous mixture is applied as a surface layer. The fatigue performance evaluation of the designed porous mixture represented the main contribution of this work. The porous mixture fatigue curve obtained

(Figure 13) proved that a highly modified asphalt such as HiMA can result in porous mixtures with outstanding performance.

Zhang et al. [36] evaluated the fatigue resistance of porous mixtures with SBS. They concluded that the modified asphalt contributed to increased stiffness, with 4.5% of asphalt content resulting in a modulus of 3097 MPa, 6.0% of 3227 MPa, and 7.5% of 3279 MPa. The increase in SBS content also enhanced the fatigue life, which was attributed to the fact that SBS made the mixtures more elastic, and the fatigue performance was improved. However, for 7.5% SBS asphalt, the SBS content increment of 1.5% only resulted in a roughly 20% increment in fatigue life. Kim et al. [85] produced porous asphalt mixtures with carbon fibre reinforcement polymer grids and obtained a fatigue life that increased by 23% to 27%. Wu et al. [18] compared the durability of porous asphalt mixtures with epoxy-modified and SBS-produced. The authors found that epoxy porous mixtures were more durable than SBS ones regarding Cantabro loss and fatigue life.

Concerning dense mixtures, research suggested that the 40 mm thickness of the porous mixture surface layer is equivalent to the structural capability of 20 mm dense mixtures [86]. For an urban road case study, the Porous asphalt mixture thickness required as a function of ESALs was estimated (Figure 14), and a pavement structure was designed (Figure 15). It can be affirmed that the porous mixture as a surface layer could be applied under elevated load traffic conditions and tends to perform similarly to dense mixtures.

In order to demonstrate the fatigue resistance achieved by the porous mixture, a comparison was made with a dense mixture produced using SBS [69], in which the test conditions were the same. Figure 16 shows the curves, and the superior fatigue performance of the porous mixture compared to the dense-graded one can be noted. Even though the dense mixture presented fewer voids (4.5%) and a higher resilient modulus (3184 MPa), preferable for fatigue resistance, the porous mixture performed better, indicating that HiMA contributed to improving the ability of the porous mixture to be damaged by fatigue. On the other hand, despite the significant improvements associated with HiMA, the high costs of this asphalt must be considered according to the project type, local conditions, and traffic.

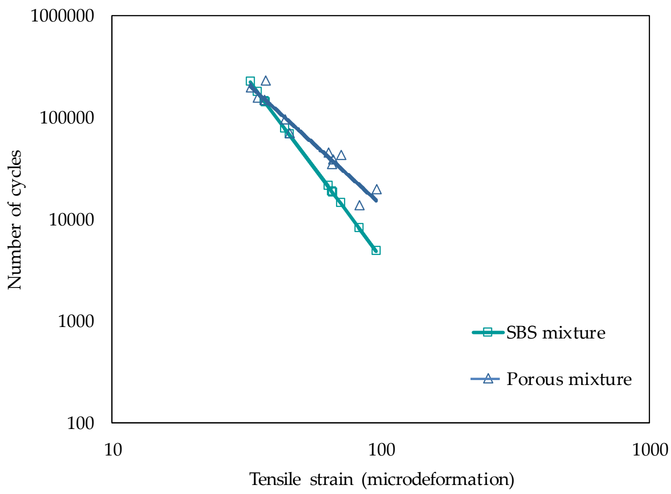

Figure 16. Comparison of fatigue curves.

Despite the fatigue resistance improvements, the results were obtained in the laboratory, and the field evaluation is necessary to validate the performance under heavy truck traffic. On the other hand, urban roads appear to be a suitable place for permeable pavement (without infiltration) application.

Thus, a case study was conducted on an urban road, which was chosen for the following reasons: (i) it borders the sea and a mangrove; (ii) it represents an adequate place for urban pervious area enlargement; and (iii) the stormwater runoff is directly released into the environment without any pollutants measurement or control.

The urban road paved area corresponds to 147,000 m^2 (extension 7000 m, six lanes with a width of 3.50 m). This study did not consider paved bike paths and sidewalks (adjacent to the road) as permeable areas. The traffic mainly comprises passenger vehicles, but heavy trucks and buses travel daily, resulting in medium traffic (estimated ESAL of 2×10^6). For this case study, a pavement structure using the porous mixture as a surface layer was designed, for which the benefits related to resistance (fatigue) and heavier traffic conditions were demonstrated.

The infiltration efficiency result (90%) corroborates that the porous mixture's absorptive capacity could promote less stormwater surface accumulation and decrease runoff pollutants concentrations. It is important to emphasise that for this case study, the stormwater is directed to the gutter and released into the sea and the mangrove. Replacing the impermeable surface with a porous mixture could be a friendly alternative for reducing contamination in such places. This urban road with a porous mixture surface layer can also minimise stormwater discharge, relieve the drainage elements' charge, and reduce frequent flood events (Figure 5). Permeable pavements will not solve all problems related to urban drainage management, but they can be considered a good alternative.

James [87] affirmed that, due to highway traffic, pavement surfaces represent one of the largest sources of pollutants. During precipitation, the runoff pollutants are charged into lakes, rivers, streams, and seas, negatively affecting the environment. This work also assessed the porous mixture's ability to reduce runoff pollutants. As for stormwater runoff pollutants, on average, the porous mixture could reduce total phosphorus concentrations, suspended solids, and faecal coliforms. On the other hand, a negative performance was observed for ammoniacal nitrogen, which increased. Variations between increase and reduction were noted for nitrate, nitrite, and chemical oxygen demand concentrations (Table S4—Supplementary Data).

Previous studies have demonstrated the benefits of permeable pavements in filtering stormwater pollutants [88–92]. Permeable pavements were effective in pollutant reduction for suspended solids (59%), lead (84%), cadmium (77%), and zinc (73%) [93]. It is important to emphasise that all permeable pavement layers contributed to stormwater filtering in the related studies. In this work, the porous mixture, isolated, showed a potential ability to reduce stormwater pollutants in runoff.

The porous asphalt mixture surface was designed to obtain the required fatigue resistance for high urban road traffic. The benefits of runoff reduction and associated pollutants by replacing impervious pavement with a porous mixture were also evaluated. However, the limitations of this work were listed. This study presented results obtained from laboratory tests and models. Experimental sections in the field must be performed for data validation and calibration. In addition, the complete analysis also comprises rutting resistance, ageing and moisture actions, and clogging. The simulations related to rain intensity to evaluate the runoff reduction have to be performed to prove the porous mixture's efficiency.

6. Conclusions

Porous asphalt mixtures can be used for multiple purposes, but sometimes their use is restricted due to a lack of mechanical behaviour evaluation, such as fatigue resistance. Thus, mechanical resistance improvement can contribute to disseminating the use, and one of the benefits is to enlarge permeable surface areas. In this work, the fatigue resistance of a porous mixture was evaluated, and the main conclusions from the study were as follows.

For porous mixtures, in asphalt content selection, beyond the usual test achievements, such as void content, interconnected voids, permeability coefficient, and Cantabro, it is important to consider the moisture-induced damage test results. Using a highly modified asphalt with SBS (HiMA) influenced the porous mixture's resilient modulus increase and contributed to better fatigue performance. According to the fatigue test results, by increasing the surface layer thickness, the designed porous mixture could be applied under heavier traffic conditions.

The infiltration efficiency result (90%) shows that the porous mixture's infiltration capacity could promote less stormwater surface accumulation and relieve the drainage elements' charge, reducing floods.

As for stormwater runoff pollutants, on average, the porous mixture contributed to total phosphorus concentrations, suspended solids, and faecal coliform reductions, except for ammoniacal nitrogen, which increased. Concentration variations were observed for chemical oxygen demand, nitrate, and nitrite.

The paving of traffic lanes with porous mixtures and the consequent increase in permeable areas can significantly contribute to the balance of the hydrological cycle and urban drainage management. However, porous mixtures as pavement surface layers represent only an alternative, and urban drainage systems must be adequate and efficient.

This work was meant to fill part of a gap in predicting porous mixtures' fatigue performance. However, studies in the field must be performed to validate the laboratory results. More investigations on other parameters affecting porous mixtures, such as rutting, clogging, and ageing, must be conducted to comprehend these mixtures' behaviour better. In addition, this work showed the possibility of rising mechanical resistance in the porous mixture produced with modified asphalt, which can help popularise and expand its use for various purposes.

Supplementary Materials: The following supporting information can be downloaded at: https://www.mdpi.com/article/10.3390/w15162962/s1, Figure S1: Compacted samples; Table S1: Crush aggregate (9.5 mm) characterization tests results [94]; Table S2: Water quality limits for non-potable purposes (Based on [68]); Table S3. Measurements to evaluate the porous mixture infiltration efficiency; Table S4. Water quality evaluation collected from stormwater runoff (road) and filtered through the porous mixture slab; Table S5. Soil (subgrade layer) characteristics [75].

Author Contributions: Conceptualization, G.H. and L.P.T.; methodology, G.H.; formal analysis, L.P.T.; investigation, G.H.; writing—original draft preparation, L.P.T.; writing—review and editing, L.P.T.; supervision, L.P.T. All authors have read and agreed to the published version of the manuscript.

Funding: This research received external funding to the first author as a scholarship, funded by the National Council for Scientific and Technological Development (CNPq) No. 432588/2016-7 and by the Co-ordination of Superior Level Staff Improvement—Brazil (CAPES)—Finance Code 001.

Informed Consent Statement: Not applicable.

Data Availability Statement: Not applicable.

Conflicts of Interest: The authors declare no conflict of interest.

References

1. Qian, Q.; Eslamian, S. Impact of urbanization on flooding. In *Flood Handbook*, 1st ed.; Eslamian, S., Eslamian, F.A., Eds.; CRC Press: Boca Raton, FL, USA, 2022; Volume 1, pp. 97–112. [CrossRef]
2. Associação Brasileira de Cimento Portland (ABCP) [Brazilian Portland Cement Association]. Projeto técnico: Pavimento permeável [Technical project: Permeable pavement]. In *Projeto Soluções para Cidades*; Associação Brasileira de Cimento Portland (ABCP): São Paulo, SP, Brazil, 2013. Available online: https://www.solucoesparacidades.com.br/wp-content/uploads/2013/10/AF_Pav%20Permeavel_web.pdf (accessed on 4 May 2023). (In Portuguese)
3. Ottoni, A.B.; Mattos, F.C.C.S. Análise crítica da obra do reservatório de amortecimento ("Piscinão") da Praça Niterói, Rio de Janeiro-RJ e proposição de soluções com sustentabilidade ambiental para o controle das inundações na região [Critical analysis of the work on the damping reservoir ("Piscinão") at Praça Niterói, Rio de Janeiro-RJ and proposition of environmentally sustainable solutions for flood control in the region]. *Rev. Cient. ANAP Bras.* **2018**, *11*, 108–122. (In Portuguese) [CrossRef]
4. Millington, N. Stormwater Politics: Flooding, Infrastructure, and Urban Political Ecology in São Paulo, Brazil. *Water Altern.* **2021**, *14*, 866–885. Available online: https://www.water-alternatives.org/index.php/alldoc/articles/vol14/v14issue3/648-a14-3-11/file (accessed on 18 April 2023).
5. Singer, M.N.; Hamouda, M.A.; El-Hassan, H.; Hinge, G. Permeable pavement systems for effective management of stormwater quantity and quality: A bibliometric analysis and highlights of recent advancements. *Sustainability* **2022**, *14*, 13061. [CrossRef]
6. Imran, H.M.; Akib, S.; Karim, M.R. Permeable pavement and stormwater management systems: A review. *Environ. Technol.* **2013**, *34*, 2649–2656. [CrossRef]

7. Hammes, G.; Thives, L.P.; Ghisi, E. Application of stormwater collected from porous asphalt pavements for non-potable uses in buildings. *J. Environ. Manag.* **2018**, *222*, 338–347. [CrossRef]
8. Zhu, H.; Yu, M.; Zhu, J.; Lu, H.; Cao, R. Simulation study on effect of permeable pavement on reducing flood risk of urban runoff. *Int. J. Transp. Sci. Technol.* **2019**, *8*, 373–382. [CrossRef]
9. Suripin, S.; Sachro, S.S.; Atmojo, P.S.; Edhisono, S.; Budieny, H.; Kurniani, D. Reducing stormwater runoff from parking lot with permeable pavement. In Proceedings of the 3rd International Conference on Energy, Environmental and Information System, Semarang, Indonesia, 14–15 August 2018; Volume 73. [CrossRef]
10. Shafique, M.; Kim, R.; Kyung-Ho, K. Rainfall runoff mitigation by retrofitted permeable pavement in an urban area. *Sustainability* **2018**, *10*, 1231. [CrossRef]
11. Infante, S.; Mobilia, M.; Longobardi, A.; Albini, M. Permeable pavements hydraulic modelling: An experimental study. *Open J. Civ. Eng.* **2021**, *15*, 266–278. [CrossRef]
12. Kuruppu, U.; Rahman, A.; Rahman, M.A. Permeable pavement as a stormwater best management practice: A review and discussion. *Environ. Earth Sci.* **2019**, *78*, 327. [CrossRef]
13. Motamedi, M.; Shafabakhsh, G.; Azadi, M. Evaluation of fatigue and rutting properties of asphalt binder and mastic modified by synthesized polyurethane. *J. Traffic Transp. Eng.* **2021**, *8*, 1036–1048. [CrossRef]
14. Yang, S.; Park, H.; Baek, C. Fatigue cracking characteristics of asphalt pavement structure under aging and moisture damage. *Sustainability* **2023**, *15*, 4815. [CrossRef]
15. Huang, Y.H. *Pavement Analysis and Design*, 2nd ed.; Prentice Hall: Upper Saddle River, NJ, USA, 2004.
16. Shadman, M.; Ziari, H. Laboratory evaluation of fatigue life characteristics of polymer modified porous asphalt: A dissipated energy approach. *Const. Build. Mater.* **2017**, *138*, 434–440. [CrossRef]
17. Sudarsanan, N.; Kim, Y.R. A critical review of the fatigue life prediction of asphalt mixtures and pavements. *J. Traffic Transp. Eng.* **2022**, *9*, 808–835. [CrossRef]
18. Wu, J.P.; Herrington, P.R.; Alabaster, D. Long-term durability of epoxy-modified open-graded porous asphalt wearing course. *Int. J. Pavement Eng.* **2019**, *20*, 920–927. [CrossRef]
19. Dan, H.-C.; Wang, Z.; Cao, W.; Liu, J. Fatigue characterization of porous asphalt mixture complicated with moisture damage. *Const. Build. Mater.* **2021**, *303*, 124525. [CrossRef]
20. Omar, H.A.; Yusoff, N.I.M.; Mubaraki, M.; Ceylan, H. Effects of moisture damage on asphalt mixtures. *J. Traffic Transp. Eng.* **2020**, *7*, 600–628. [CrossRef]
21. Poulikakos, L.D.; Partl, M.N. Evaluation of moisture susceptibility of porous asphalt concrete using water submersion fatigue tests. *Constr. Build. Mater.* **2009**, *23*, 3475–3484. [CrossRef]
22. Wu, J.; Wang, Y.; Liu, Q.; Wang, Y.; Ago, C.; Oeser, M. Investigation on mechanical performance of porous asphalt mixtures treated with laboratory aging and moisture actions. *Constr. Build. Mater.* **2020**, *238*, 117694. [CrossRef]
23. Zhang, K.; Liu, Y.; Nassiri, S.; Li, H.; Englund, K. Performance evaluation of porous asphalt mixture enhanced with high dosages of cured carbon fiber composite materials. *Constr. Build. Mater.* **2021**, *274*, 122066. [CrossRef]
24. Ndon, U.J. Trends in the application of permeable pavement as sustainable highway storm water management option for safe-use of roadways. *J. Civil. Environ. Eng.* **2017**, *7*, 1000288. [CrossRef]
25. Haryati, Y.; Norhidayah, A.H.; Nordiana, M.; Juraidah, A.; Nor Hayati, A.H.; Ramadhansyah, P.J.; Khairil Azman, M.; Haryati, A. Stability and rutting resistance of porous asphalt mixture incorporating coconut shells and fibres. *IOP Conf. Ser. Earth Environ. Sci.* **2019**, *244*, 012043. [CrossRef]
26. Wang, S.; Kang, A.; Xiao, P.; Li, B.; Fu, W. Investigating the effects of chopped basalt fiber on the performance of porous asphalt mixture. *Adv. Mat. Sci. Eng.* **2019**, *2019*, 2323761. [CrossRef]
27. Gupta, A.; Rodriguez-Hernandez, J.; Castro-Fresno, D. Incorporation of additives and fibers in porous asphalt mixtures: A review. *Materials* **2019**, *12*, 3156. [CrossRef] [PubMed]
28. Senior-Arrieta, V.; Córdoba-Maquilón, J.E. Mechanical characterization of porous asphalt mixes modified with fatty acid amides-FAA. *Ing. Investig.* **2017**, *37*, 43–48. [CrossRef]
29. Li, X.; Shen, J.; Ling, T.; Yuan, F. Fatigue properties of aged porous asphalt mixtures with an epoxy asphalt binder. *J. Mater. Civ. Eng.* **2022**, *34*, 04021488. [CrossRef]
30. Lin, C.; Tongjing, W.; Le, T.; Junjie, Y.; Jiachen, S. Laboratory evaluation on performance of porous polyurethane mixtures and OGFC. *Const. Build. Mater.* **2018**, *169*, 436–442. [CrossRef]
31. Garcia, E.S.H.; Thives, L.P.; Ghisi, E.; Antunes, L.N. Analysis of permeability reduction in drainage asphalt mixtures due to decrease in void volume. *J. Clean. Prod.* **2020**, *248*, 119292. [CrossRef]
32. Shirini, B.; Imaninasa, R. Performance evaluation of rubberized and SBS modified porous asphalt mixtures. *Const. Build. Mater.* **2016**, *107*, 165–171. [CrossRef]
33. Huang, W.; Liu, X.; Zhang, S.; Zheng, Y.; Ding, Q.; Tong, B. Performance-guided design of permeable asphalt concrete with modified asphalt binder using crumb rubber and SBS modifier for sponge cities. *Materials* **2021**, *14*, 1266. [CrossRef]
34. Chen, S.; Gu, L.; Tu, Z.; Ma, T.; Kang, L. Mechanical properties of porous asphalt mixtures containing styrene-butadiene-styrene and high-viscosity modifiers. *J. Mater. Civ. Eng.* **2023**, *35*, 04022417. [CrossRef]
35. Willis, J.R.; Timm, D.H.; Kluttz, R. Performance of a highly polymer-modified asphalt binder test section at the national center for asphalt technology pavement test track. *Transp. Res. Rec.* **2016**, *2575*, 1–9. [CrossRef]

36. Zhang, J.; Huang, W.; Hao, G.; Yan, C.; Lv, Q.; Cai, Q. Evaluation of open-grade friction course (OGFC) mixtures with high content SBS polymer modified asphalt. *Const. Build. Mater.* **2021**, *270*, 121374. [CrossRef]
37. Hamzah, M.O.; Hasan, M.M.; Van Bochove, G. Rational control parameters for determination of design binder content of porous asphalt. In Proceedings of the 5th Eurasphalt & Eurobitume Congress, Istanbul, Turkey, 13–15 June 2012.
38. Kolodziej, V.M. Estudo das Propriedades Acústicas, Drenantes e Mecânicas de Revestimentos Asfálticos Porosos [Study of the Acoustic, Draining and Mechanical Properties of Porous Asphalt Surfaces]. Master's Thesis, Universidade Federal de Santa Catarina, Programa de Pós-Graduação em Engenharia Civil, Florianópolis, Brazil, 17 October 2016. (In Portuguese)
39. Ji, T.; Xiao, L.; Chen, F. Parametric analysis of the drainage performance of porous asphalt pavement based on a 3D FEM method. *J. Mater. Civ. Eng.* **2020**, *32*, 04020383. [CrossRef]
40. *ASTM D7064*; Standard Practice for Open-Graded Friction Course (OGFC) Mix Design. American Society for Testing and Materials (ASTM): West Conshohocken, PA, USA, 2003.
41. *DNER-ES 386*; Pavimentação–Pré-Misturado a Quente com Asfalto Polímero–Camada Porosa de Atrito–Especificação de Serviço [Paving–Hot Premixed with Polymer Asphalt–Porous Friction Layer–Specification]. Departamento Nacional de Infraestrutura de Transportes (DNIT), Diretoria de Planejamento e Pesquisa/IPR: Rio de Janeiro, RJ, Brazil, 1999. (In Portuguese)
42. Zanoletti, A.; Botempi, E. Editorial: Urban runoff of pollutants and their treatment. *Front. Environ. Chem.* **2023**, *4*, 1151859. [CrossRef]
43. Müller, A.; Österlund, H.; Marsalek, J.; Viklander, M. The pollution conveyed by urban runoff: A review of sources. *Sci. Total Environ.* **2020**, *709*, 136125. [CrossRef]
44. Piñon-Colin, T.J.; Rodriguez-Jimenez, R.; Rogel-Hernandez, E.; Alvarez-Andrade, A.; Wakida, F.T. Microplastics in stormwater runoff in a semiarid region, Tijuana, Mexico. *Sci. Total Environ.* **2020**, *704*, 135411. [CrossRef]
45. Tota-Maharaj, K.; Scholz, M. Efficiency of permeable pavement systems for the removal of urban runoff pollutants under varying environmental conditions. *Environ. Prog. Sustain. Energy* **2010**, *33*, 676–680. [CrossRef]
46. Antunes, L.N.; Thives, L.P.; Ghisi, E. Potential for potable water savings in buildings by using stormwater harvested from porous pavements. *Water* **2016**, *8*, 110. [CrossRef]
47. Thives, L.P.; Ghisi, E.; Brecht, D.G.; Pires, D.M. Filtering capability of porous asphalt pavements. *Water* **2018**, *10*, 206. [CrossRef]
48. Alam, T.; Mahmoud, A.; Jones, K.D.; Bezares-Cruz, J.C.; Guerrero, J. A comparison of three types of permeable pavements for urban runoff mitigation in the semi-arid South Texas, USA. *Water* **2019**, *11*, 1992. [CrossRef]
49. Ghisi, E.; Belotto, T.; Thives, L.P. The Use of permeable interlocking concrete Pavement to filter stormwater for non-potable uses in buildings. *Water* **2020**, *12*, 2045. [CrossRef]
50. Liu, J.; Yan, H.; Liao, Z.; Zhang, K.; Schimidt, A.; Tao, T. Laboratory analysis on the surface runoff pollution reduction performance of permeable pavements. *Sci. Total Environ.* **2019**, *692*, 1–8. [CrossRef]
51. Liu, J.; Li, H.; Yang, B.; Xie, N.; Ning, Y. Laboratory investigation on pollutant removal effect of purification materials for porous asphalt pavement. *Transp. Res. Rec.* **2022**, *2676*, 421–435. [CrossRef]
52. Lu, Q.; Fu, P.C.; Harvey, J.T. *Laboratory Evaluation of the Noise and Durability Properties of Asphalt Surface Mixes*; Research Report No, UCPRC-RR-2009-07; University of California, Pavement Research Center: Davis/Berkeley, CA, USA, 2009; Available online: https://escholarship.org/uc/item/2sq561kp (accessed on 20 April 2023).
53. *DNIT 129*; Cimento Asfáltico de Petróleo Modificado por Polímero Elastomérico–Especificação de Material [Polymer-Modified Petroleum Asphalt Cement Elastomeric–Material Specification]. Departamento Nacional de Infraestrutura de Transportes (DNIT), Diretoria de Planejamento e Pesquisa/IPR: Rio de Janeiro, RJ, Brazil, 2011. (In Portuguese)
54. *NBR 6576*; Materiais Asfálticos–Determinação da Penetração [Bituminous Materials–Determination of Penetration]. Associação Brasileira de Normas Técnicas (ABNT): São Paulo, SP, Brazil, 2007. (In Portuguese)
55. *NBR 6560*; Materiais Asfálticos–Determinação do Ponto de Amolecimento–Método do anel e bola [Bituminous Materials–Determination of the Softening Point–Ring-and-Ball Method]. Associação Brasileira de Normas Técnicas (ABNT): São Paulo, SP, Brazil, 2016. (In Portuguese)
56. *NBR 15086*; Materiais betuminosos–Determinação da Recuperação Elástica pelo Ductilômetro de Cimentos Asfálticos Modificados por Polímeros Elastoméricos ou Borracha [Bituminous Materials–Determination of the Elastic Recovery by Ductilometer of Elastomeric Polymer and Ground Tyre Modified Asphalt]. Associação Brasileira de Normas Técnicas (ABNT): São Paulo, SP, Brazil, 2022. (In Portuguese)
57. *NBR 15184*; Materiais betuminosos–Determinação da Viscosidade em Temperaturas Elevadas Usando um Viscosímetro Rotacional [Bituminous Materials–Viscosity Determination of Elevated Temperatures Using a Rotational Viscometer]. Associação Brasileira de Normas Técnicas (ABNT): São Paulo, SP, Brazil, 2021. (In Portuguese)
58. *NBR 15166*; Asfalto Modificado–Ensaio de Separação de Fase [Modified Asphalt–Test Method for Phase Separation]. Associação Brasileira de Normas Técnicas (ABNT): São Paulo, SP, Brazil, 2004. (In Portuguese)
59. *NBR 15235*; Materiais Asfálticos–Determinação do Efeito do calor e do Ar em uma Película Delgada Rotacional [Asphalt Materials–Determination of Effect of heat and Air on a Moving Thin-Film]. Associação Brasileira de Normas Técnicas (ABNT): São Paulo, SP, Brazil, 2009. (In Portuguese)
60. *ASTM D3203*; Standard Test Method for Percent Air Voids in Compacted Asphalt Mixtures. American Society for Testing and Materials (ASTM): West Conshohocken, PA, USA, 2017.

61. *AFNOR NF P98-254-2*; Mesure de Proprietés Liées à la Perméabilité des Matériaux des Mélanges Hydrocarbonés, Partie 2. Association Française de Normalisation (AFNOR): Paris, France, 1993. (In French)
62. Raimbault, G.; Andrieu, H.; Berthier, E.; Joannis, C.; Legret, M. Infiltration des eaux Pluviales à Travers les Surfaces Urbaines: Des Revêtements Imperméables aux Structures-Réservoirs. *Bull. Des. Lab. Des. Ponts Chaussées* **2002**, *238*, 39–50. Available online: https://www.ifsttar.fr/collections/BLPCpdfs/blpc_238_39-50.pdf (accessed on 12 February 2023). (In French)
63. *NLT-327*; Permeabilidad In Situ de Pavimentos Drenantes con el Permeámetro LCS. Laboratorio Escuela de Caminos de Santander: Santander/Cantabria, Spain, 2000; In Spanish. Available online: http://normativa.itafec.com/ensayos/ES.12.02.138.LT.pdf (accessed on 12 March 2023).
64. *Tex-245-F*; Test Procedure of Cantabro Loss. Texas Department of Transportation: Austin, TX, USA, 2021. Available online: https://ftp.dot.state.tx.us/pub/txdot-info/cst/TMS/200-F_series/pdfs/bit245.pdf (accessed on 25 April 2023).
65. *AASHTO T 283*; Resistance of Compacted Asphalt Mixtures to Moisture-Induced Damage. American Association of State and Highway Transportation Officials: Washington, DC, USA, 2021.
66. *DNIT 135*; Pavimentação Asfáltica-Misturas Asfálticas–Determinação do Módulo de Resiliência–Método de Ensaio [Asphalt Paving–Asphalt Mixtures-Resilient Modulus Determination–Test Method]. Departamento Nacional de Infraestrutura de Transportes (DNIT), Diretoria de Planejamento e Pesquisa/IPR: Rio de Janeiro, RJ, Brazil, 2018. (In Portuguese)
67. *DNIT 183*; Pavimentação Asfáltica-Ensaio de Fadiga por Compressão Diametral à Tensão Controlada–Método de Ensaio [Asphalt Paving-Diametral Fatigue Test by Controlled Force Indirect Tensile–Test Method]. Departamento Nacional de Infraestrutura de Transportes (DNIT), Diretoria de Planejamento e Pesquisa/IPR: Rio de Janeiro, RJ, Brazil, 2018. (In Portuguese)
68. ANA. *Conservação e Reúso da Água em Edificações [Water Conservation and Reuse in Buildings]*; Agência Nacional De Águas: São Paulo, SP, Brazil, 2005; (In Portuguese). Available online: https://smastr16.blob.core.windows.net/municipioverdeazul/2011/11/ManualConservacaoReusoAguaEdificacoes.pdf (accessed on 10 January 2023).
69. *Software MeDiNa*; Departamento Nacional de Infraestrutura de Transportes (DNIT), Diretoria de Planejamento e Pesquisa/IPR: Rio de Janeiro, RJ, Brazil, 2020; (In Portuguese). Available online: https://www.gov.br/dnit/pt-br/assuntos/planejamento-e-pesquisa/ipr/medina (accessed on 16 May 2023).
70. INMET. *Normais Climatológicas do Brasil [Climatological Standards in Brazil]*; Instituto Nacional de Meteorologia (INMET): Brasília, DF, Brazil, 2023. Available online: https://portal.inmet.gov.br/normais (accessed on 18 March 2023). (In Portuguese)
71. INMET. 2023. Available online: https://portal.inmet.gov.br/dadoshistoricos (accessed on 18 March 2023). (In Portuguese)
72. INMET. 2023. Available online: https://tempo.inmet.gov.br/ValoresExtremos/PMAX (accessed on 18 March 2023). (In Portuguese)
73. ND. 2022. Available online: https://ndmais.com.br/tempo/chuvas-causam-alagamentos-e-deslizamento-em-florianopolis/ (accessed on 27 December 2022). (In Portuguese)
74. Simm Júnior, G.P. Estudo do Comportamento de Estruturas de Pavimentos com Materiais Alternativos Visando a Redução dos Custos de Pavimentação no Estado de Santa Catarina [The Behaviour of Pavement Structures Study with Alternative Materials Aiming Paving Costs Reducing in the State of Santa Catarina]. Master's Thesis, Universidade Federal de Santa Catarina, Florianópolis, SC, Brazil, 2007. (In Portuguese)
75. Custódio, D.A.S.; Pascoal, P.T.; Baroni, M.; Pereira, D.S.; Specht, L.P. Influência da Saturação pós-Compactação no Comportamento Resiliente de um solo Laterítico Empregado em Subleito Rodoviário. *Rev. Ibero Am. Ciências Ambient.* **2021**, *12*, 265–278. (In Portuguese) [CrossRef]
76. U.S. Environmental Protection Agency (EPA). EnviroAtlas. Available online: https://enviroatlas.epa.gov/enviroatlas/DataFactSheets/pdf/ESC/Percentimperviousareacensusblockgroup.pdf (accessed on 25 January 2023).
77. Pasquier, U.; Vahmani, P.; Jones, A.D. Quantifying the city-scale impacts of impervious surfaces on groundwater recharge potential: An urban application of WRF–Hydro. *Water* **2022**, *14*, 3134. [CrossRef]
78. Strohbach, M.W.; Döring, A.O.; Möck, M.; Sedrez, O.; Munn, O.; Schneider, A.K.; Weber, S.; Schröder, B. The "Hidden Urbanization": Trends of impervious surface in low-density housing developments and resulting impacts on the water balance. *Front. Environ. Sci.* **2019**, *7*, 29. [CrossRef]
79. Clar, M.L.; Barfield, B.J.; O'Connor, T.P. *Stormwater Best Management Practice Design Guide: Volume 1, General Considerations*; Report EPA/600/R-04/121; Environmental Protection Agency (EPA): Cincinnati, OH, USA, 2004. Available online: https://nepis.epa.gov/Exe/ZyPDF.cgi/901X0A00.PDF?Dockey=901X0A00.PDF (accessed on 15 May 2023).
80. Minnesota Pollution Control Agency. Overview for Permeable Pavement. Available online: https://stormwater.pca.state.mn.us/index.php/Overview_for_permeable_pavement (accessed on 26 January 2023).
81. United States Geological Survey (USGS). Evaluating the Potential Benefits of Permeable Pavement on the Quantity and Quality of Stormwater Runoff. Available online: https://www.usgs.gov/centers/upper-midwest-water-science-center/science/evaluating-potential-benefits-permeable-pavement (accessed on 11 January 2023).
82. Huang, W.; Yu, H.; Lin, Y.; Zheng, Y.; Ding, Q.; Tong, B.; Wang, T. Energy analysis for evaluating durability of porous asphalt mixture. *Constr. Build. Mater.* **2022**, *326*, 126819. [CrossRef]
83. Jaya, R.P.; Hamzah, M.O. Properties of porous asphalt mixture made with styrene butadiene styrene under long term oven ageing. *Adv. Mater. Res.* **2012**, *486*, 378–383. Available online: http://www.scientific.net/AMR.486.378 (accessed on 27 July 2023).
84. Shukry, A.M.S.; Hassan, N.A.; Hainin, M.R.; Abdullah, M.E.; Abdullah, N.A.M.; Mahmud, M.Z.H. Experimental evaluation of anti-stripping additives on porous asphalt mixtures. *J. Teknol.* **2016**, *78*, 113–119. [CrossRef]

85. Kim, H.; Sokolov, K.; Poulikakos, L.D.; Partl, M.N. Fatigue evaluation of porous asphalt composites with carbon fiber reinforcement polymer grids. *Transp. Res. Rec.* **2009**, *2116*, 108–117. [CrossRef]
86. Potter, J.G.; Halliday, A.R. *The Contribution of Pervious Macadam Surfacing to the Structural Performance of Roads*; TRL Report 1022; Transport Research Laboratory: Crowthorne, UK, 1981.
87. James, E. A Literature review on the effect of porous asphalt roads on water pollution. In *Sustainable Road Surfaces for Traffic Noise Control*; Silvia Project Report; European Commission: Ottawa, ON, Canada, 2013.
88. Pratt, C.J.; Mantle, J.D.G.; Schofield, P.A. UK research into the performance of permeable pavement, reservoir structures in controlling stormwater discharge quantity and quality. *Water Sci. Technol.* **1995**, *32*, 63–69. [CrossRef]
89. Gilbert, J.K.; Clausen, J.C. Stormwater runoff quality and quantity from asphalt, paver, and crushed stone driveways in Connecticut. *Water Res.* **2006**, *40*, 826–832. [CrossRef]
90. Sansalone, J.; Kuang, X.; Ying, G.; Ranieri, V. Filtration and clogging of permeable pavement loaded by urban drainage. *Water Res.* **2012**, *46*, 6763–6774. [CrossRef] [PubMed]
91. Park, D.G.; Sandoval, N.; Lin, W.; Kim, H.; Cho, Y.H. A case study: Evaluation of water storage capacity in permeable block pavement. *KSCE J. Civ. Eng.* **2014**, *18*, 514–520. [CrossRef]
92. Knappenberger, T.; Jayakaran, A.D.; Stark, J.D.; Hinman, C.H. Monitoring porous asphalt stormwater infiltration and outflow. *J. Irrig. Drain. Eng.* **2017**, *143*, 04017027. [CrossRef]
93. Legret, M.; Colandini, V. Effects of a porous pavement with reservoir structure on runoff water: Water quality and fate of heavy metals. *Water Sci. Technol.* **1999**, *39*, 111–117. [CrossRef]
94. *ASTM C88*; Standard Test Method for Soundness of Aggregates by Use of Sodium Sulfate or Magnesium Sulfate. American Society for Testing and Materials (ASTM): West Conshohocken, PA, USA, 2018.